



**Power Spectral Densities of Atmospheric  
Aerosol Particle Counts**

**by Chatt C. Williamson, Steven C. Hill, Dennis M. Garvey,  
Michael L. Larsen, and Cheryl L. Klipp**

**ARL-TR-5064**

**January 2010**

## **NOTICES**

### **Disclaimers**

The findings in this report are not to be construed as an official Department of the Army position unless so designated by other authorized documents.

Citation of manufacturer's or trade names does not constitute an official endorsement or approval of the use thereof.

Destroy this report when it is no longer needed. Do not return it to the originator.

# **Army Research Laboratory**

Adelphi, MD 20783-1197

---

---

**ARL-TR-5064**

**January 2010**

## **Power Spectral Densities of Atmospheric Aerosol Particle Counts**

**Chatt C. Williamson, Steven C. Hill, Dennis M. Garvey,  
Michael L. Larsen, and Chrryl L. Klopp  
Computational and Information Sciences Directorate, ARL**

REPORT DOCUMENTATION PAGE			Form Approved OMB No. 0704-0188		
Public reporting burden for this collection of information is estimated to average 1 hour per response, including the time for reviewing instructions, searching existing data sources, gathering and maintaining the data needed, and completing and reviewing the collection information. Send comments regarding this burden estimate or any other aspect of this collection of information, including suggestions for reducing the burden, to Department of Defense, Washington Headquarters Services, Directorate for Information Operations and Reports (0704-0188), 1215 Jefferson Davis Highway, Suite 1204, Arlington, VA 22202-4302. Respondents should be aware that notwithstanding any other provision of law, no person shall be subject to any penalty for failing to comply with a collection of information if it does not display a currently valid OMB control number. <b>PLEASE DO NOT RETURN YOUR FORM TO THE ABOVE ADDRESS.</b>					
1. REPORT DATE (DD-MM-YYYY) January 2010		2. REPORT TYPE Final		3. DATES COVERED (From - To) FY08–FY09	
4. TITLE AND SUBTITLE Power Spectral Densities of Atmospheric Aerosol Particle Counts			5a. CONTRACT NUMBER		
			5b. GRANT NUMBER		
			5c. PROGRAM ELEMENT NUMBER		
6. AUTHOR(S) Chatt C. Williamson, Steven C. Hill, Dennis M. Garvey, Michael L. Larsen, and Cheryl L. Klipp			5d. PROJECT NUMBER		
			5e. TASK NUMBER		
			5f. WORK UNIT NUMBER		
7. PERFORMING ORGANIZATION NAME(S) AND ADDRESS(ES) U.S. Army Research Laboratory Attn: RDRL-CIE-D 2800 Powder Mill Road Adelphi, MD 20783-1197			8. PERFORMING ORGANIZATION REPORT NUMBER ARL-TR-5064		
9. SPONSORING/MONITORING AGENCY NAME(S) AND ADDRESS(ES)			10. SPONSOR/MONITOR'S ACRONYM(S)		
			11. SPONSOR/MONITOR'S REPORT NUMBER(S)		
12. DISTRIBUTION/AVAILABILITY STATEMENT Approved for public release; distribution unlimited.					
13. SUPPLEMENTARY NOTES					
14. ABSTRACT The velocity components of the atmospheric wind typically have a power spectral density (PSD) with a slope of $-5/3$ in an “inertial subrange” of frequencies, roughly from 0.01 to $>10$ Hz depending on the wind speed and stability. As passive scalars, atmospheric temperature and humidity have a relatively small direct effect on the winds, and they also typically have a $-5/3$ slope in this frequency range. Atmospheric aerosol particles are also expected to behave as passive scalars, and PSD slopes of $-5/3$ have been reported for some atmospheric aerosol measurements with a volume-based light-scattering instrument. Herein, we present aerosol measurements obtained with a single-particle optical counter over two four-day periods with concurrent sonic anemometer measurements of wind speed and temperature. PSDs of the aerosol particle counts, temperature, and winds are presented and compared in the frequency range $10^{-4}$ to 10 Hz for 5 min subintervals. As expected, the PSDs of the velocity components and of the temperature decrease with a slope near the predicted $-5/3$ . But the slopes of the PSDs of the aerosol particle counts are near $-5/3$ for only a small fraction of the subintervals; generally the magnitude of the slopes is much smaller than $-5/3$ and often close to zero. The discrete nature of the particle counts results in a shot-noise floor, which limits the slopes in PSD that can be measured at low particle concentrations and high sample rates. Interestingly, an overall slope of $-7/6$ is found over a large frequency range when the entirety of both of the four day periods is considered.					
15. SUBJECT TERMS Power spectral density, aerosol, Welch's method, atmosphere					
16. SECURITY CLASSIFICATION OF:			17. LIMITATION OF ABSTRACT UU	18. NUMBER OF PAGES 32	19a. NAME OF RESPONSIBLE PERSON Chatt C. Williamson
a. REPORT Unclassified	b. ABSTRACT Unclassified	c. THIS PAGE Unclassified			19b. TELEPHONE NUMBER (Include area code) (301) 394-1378

Standard Form 298 (Rev. 8/98)  
Prescribed by ANSI Std. Z39.18

---

# Contents

---

<b>List of Figures</b>	<b>iv</b>
<b>1. Introduction</b>	<b>1</b>
1.1 Overview .....	1
1.2 Background .....	2
1.2.1 Turbulent Eddies .....	2
1.2.2 Spectra of Turbulence – Models and Measurements .....	2
1.2.3 Spectra of Turbulence – Passive Scalars .....	3
1.3 Approach .....	5
<b>2. Methods</b>	<b>5</b>
2.1 Experimental .....	5
2.2 Analysis .....	6
<b>3. Results and Discussion</b>	<b>7</b>
3.1 Particle Counts Measured versus Time .....	7
3.2 Power Spectral Densities of Wind, Temperature, and Aerosol for 90 h Periods .....	8
3.3 Limitations on Frequency Spectra as a Function of Particle Count (Shot Noise Floor)	10
3.4 Time-Dependence of the Slopes of the Power Spectral Densities of Wind, Temperature, and Aerosol for 5 min Intervals .....	12
3.5 Slope of Aerosol Power Spectral Densities with Low and High Aerosol Concentrations	12
<b>4. General Discussion</b>	<b>18</b>
<b>5. Summary</b>	<b>19</b>
<b>6. References</b>	<b>20</b>
<b>Appendix. Effect of Dropping 15 s of Data</b>	<b>23</b>
<b>Distribution List</b>	<b>25</b>

---

## List of Figures

---

Figure 1a. Aerosol particle counts measured at 20 Hz using the Climet particle counter during the period July 3–7, 2007. ....	8
Figure 1b. Aerosol particle counts measured at 20 Hz using the Climet particle counter, July 13–17, 2007.....	8
Figure 2. PSDs estimated using the modified Welch method for the u component of wind, the temperature ( $T_v$ ), and aerosols. The data for aerosols was binned into two different sampling frequencies before analysis. The lines with slopes of $-5/3$ (solid) and $-7/6$ (dashed) are for comparison with the winds and the aerosols, respectively. The slope of the wind (u) is similar to $-5/3$ in the inertial subrange ( $10^{-1}$ to $10^1$ Hz).....	9
Figure 3. PSDs estimated using the modified Welch method for the aerosols for the two sampling periods (July 3–7 and July 13–17, 2007). The line with slope $-7/6$ (dashed) is for comparison. ....	10
Figure 4. PSDs estimated for a 5-min sample of measured particles (blue) and for the sample after 90% (green) and then 99% (red) of the particles have been randomly eliminated. ....	11
Figure 5. Estimate of the slope of the PSDs calculated for the winds (blue), sonic temperature (green), and aerosol number concentrations (red). ....	12
Figure 6. Mean particle count of aerosols, TKE, and slope of aerosol PSD for each 5-min window of a 90 hr data collection beginning July 3, 2007. ....	13
Figure 7a. Aerosol particle concentrations measured at 20 Hz using the Climet OPC, July 3–7, 2007, during a period where the concentration is lowest. The average particle count is about 9.21 per bin.....	14
Figure 7b. Aerosol particle concentrations measured at 20 Hz using the Climet OPC, July 3–7, 2007, during a period where the concentration is highest. The average particle number is 62.8 per bin. ....	15
Figure 8. The slope of the linear fit of the PSD for a fixed frequency interval (0.05 to 1.0 Hz) and a given mean particle count.....	16
Figure 9. Right hand interval bound of the frequency interval for which the linear fit of the PSD was closest to $-5/3$ slope, with a left hand bound of 0.05 Hz and a given mean particle count.....	17
Figure 10. Right hand bound of the frequency interval for which the linear fit of the PSD is within 1% (blue), 5% (red), or 10% (green) of $-5/3$ slope, with a left hand bound of 0.05 Hz and a given mean particle count.....	18
Figure A-1. PSDs for aerosols July 13–17, 2007, with and without the zeros removed. The effect appears small.....	23
Figure A-2. Same as for figure A-1 though limiting the display to the frequency interval in the region of most significant difference for the two PSDs.....	24

---

# 1. Introduction

---

## 1.1 Overview

Atmospheric aerosols have many impacts on humans and the earth's environment, as they affect the health of humans, other animals, and plants. Both biological particles (e.g., tuberculosis, plague) and non-biological particles (e.g., asbestos, polycyclic aromatic hydrocarbons (PAH) from combustion) have important health effects. Atmospheric aerosols also affect global climate, directly by absorbing and scattering radiation and indirectly by acting as cloud condensation nuclei (CCN). They are also important in atmospheric chemistry because many atmospheric reactions occur inside or on the surfaces of particles, and agglomeration of particles as well as adsorption of gases onto the surface of particles is common. Atmospheric aerosols can affect communications and imaging through the atmosphere because of their effects on the propagation of light and other electromagnetic radiation. Because of the importance of atmospheric aerosols for many areas, and the importance of measuring and understanding aerosols (in total, and particular types of aerosols, such as biowarfare or chemical warfare agents), a better understanding of the statistics of atmospheric aerosols is desirable. The statistics of atmospheric aerosols appears to be more complex than the statistics of atmospheric turbulence—defined in terms of wind velocities—because aerosols are generated in many ways; their behavior depends strongly on size and chemical composition; and they grow, shrink, and/or age with time in ways that depend upon temperature, humidity, sunlight, and the vapor pressure of gaseous species.

The primary topics of this report are our measurements of atmospheric aerosols, counted one at a time, and our calculations of the power spectral density (PSD) of the aerosol particle counts over a large frequency range. The measurements were made at a fixed point in the atmospheric boundary layer, on the roof of a building, about 1 m from the flat surface of the roof. We achieved the very large range of frequencies (about 5 orders of magnitude) and high frequencies in the aerosol PSD by making single-particle measurements using an instrument that draws air through at 28 liters/min. One objective was to determine under what conditions and over what frequency range the aerosol PSDs calculated from counts of single-particles exhibited a  $-5/3$  slope. We also discuss and speculate about how this measured aerosol PSD might depend upon the time the added aerosol had to mix before it reached the detector; we also speculate on changes due to atmospheric chemistry and on the strength and variability of the winds.

One difficulty in discussing atmospheric turbulence is that the term “turbulence” is used differently by different researchers, where possibly the main difference pertains to the regions where the term “turbulence” applies. For example, for some researchers the regions in which turbulence occurs may be defined in terms of frequency (spectral analysis), or distance from the ground, or height within the boundary layer. Some researchers limit their definition of

“turbulence” to regions in which Kolmogorov’s assumptions for isotropic turbulence are valid (possible symmetries of the Navier-Stokes equations pertain; the turbulent flow is isotropic, self-similar, and has a non-vanishing dissipation rate per unit mass (see Frisch, 1995, Ch. 6)), i.e., to an “inertial subrange,” lying between the “energy input range” at the low frequency end and the “dissipation range” at the high end or to regions where the PSD of winds should follow a  $-5/3$  power law. Kundu (1990) quotes Marcel Lesieur as, “turbulence is a dangerous topic which is at the origin of serious fights in scientific meetings since it represents extremely different points of view, all of which have in common their complexity, as well as an inability to solve the problem. It is even difficult to agree on what exactly is the problem to be solved.” Mandelbrot (1983) asked, “Should the term ‘turbulence’ denote all unsmooth flows, including much of meteorology and oceanography? Or is it better to reserve it for a narrow class, and, if so, for which one? Each scholar seems to answer these questions differently.” In this report we use turbulence in a broader sense, and include much of meteorology and unsmooth flows.

## **1.2 Background**

### **1.2.1 Turbulent Eddies**

Turbulence is often envisioned as being composed of eddies of many sizes. Richardson (Kundu, 1990, ch. 14.2) suggested that energy is added to the atmosphere at large scales—or equivalently, into large-scale eddies—and then cascades downward into smaller eddies, and is eventually dissipated by viscous motion. That the eddy concept includes rotation is enhanced by Richardson also referring to eddies as “whorls.” Although Webster’s Dictionary defines an “eddy” as “a current of air, water, or other fluid moving against the main current and having a circular motion,” and although in everyday usage, “rotation” seems to be a fundamental aspect of an eddy, some researchers appear to envision turbulence in terms of random variations, with no initial concept of rotation. Here we will largely go with Pope’s definition (Pope, 1998): “An ‘eddy’ eludes precise definition, but is conceived to be a turbulent motion, localized within a region of size  $l$ , that is at least moderately coherent over this region.”

### **1.2.2 Spectra of Turbulence – Models and Measurements**

The power spectrum of the wind velocities in turbulence was shown theoretically by Kolmogorov (Frisch, 95) to follow a  $-5/3$  power law in an inertial subrange when several conditions apply. He assumed a homogenous, stationary, isotropic cascade process where there is no energy loss until dissipation occurs at the highest frequencies, and so the rate of energy flow from lower frequencies is a constant. There was no assumption of vortices or eddies.

Onsager (1945; 1949) began from an assumption of vortices that could interact (similar to Richardson’s initial hypotheses) and arrived at a  $-5/3$  frequency dependence. He also showed that for the 2-D case, at least, energy added to small eddies could transfer to larger eddies to take the system in the direction of the  $-5/3$  sloped PSD.



The PSD of the winds in the atmospheric boundary layer, particularly the surface layer, calculated from measured wind velocity components has in fact been observed to follow a  $-5/3$  power law over a range of frequencies, which may extend from about 0.01 to  $>10$  Hz (Frisch, 1995; Kaimal, et al; 1972; Kaimal, 1973). The extent of this range is smaller for the vertical velocity component compared to the longitudinal and transverse components, i.e., the “cutoff” on the low frequency end occurs at a higher frequency or shorter wavelength.

### 1.2.3 Spectra of Turbulence – Passive Scalars

The  $-5/3$  power law has also been suggested to apply to “passive scalars,” such as temperature and humidity (Batchelor, 1953). It is argued that passive scalars should follow the turbulence structure of the winds. Warhaft (2000), however, reporting on results of wind tunnel studies, is less supportive of the view that the PSDs of passive scalars necessarily follow a  $-5/3$  slope. A passive scalar should have no more than a very small effect on the motion of the suspending gas, and should largely follow the flow of the gas. Aerosols in the atmosphere typically have only a tiny mass compared to that of the air in which they are suspended. Also, most aerosols have small settling velocities—e.g., the settling velocity in still air for a 1 mm water droplet is 35 mm/s. Blackadar (1997) states: “Most properties other than momentum and heat are passive in the sense that their distribution plays no part in the turbulent mechanisms that spread them. Included in the broad list of such properties are most contaminants ....”, e.g., aerosols. What are the conditions, then, for which aerosols behave as passive scalars, and over what frequency ranges do spectra of their concentrations exhibit a  $-5/3$  slope?

Porch and Gillette (1977) measured a  $-5/3$  PSD for atmospheric aerosols under conditions where there were high levels of wind-blown dust, and it is not difficult to imagine that the addition of aerosols might go according to the variance of the winds that are blowing the aerosols into the air. This is the only reported measurement of a  $-5/3$  slope for atmospheric aerosols that we have found in the open literature. In this case, an eyeball alignment fits the measurement to a  $-5/3$  slope over a frequency range of 0.1 to 5 Hz. In measurements of plumes of obscurant smokes with optical particle counters, Garvey et al. (1982) found slopes of the PSDs to be about  $-5/3$  over a limited range (no more than 0.03 to 0.2 Hz). In these tests, the particle counters covered nominal size ranges of radii from 0.12 to 0.42  $\mu\text{m}$ , 0.25 to 1.0  $\mu\text{m}$ , and 0.5 to 10  $\mu\text{m}$ . There was no obvious size dependence of the measured spectra, though the number concentration in a given size interval had to be high enough to reflect the aerosol concentration at a statistically significant level. PSDs with slopes of  $-5/3$  over at least part of the frequency range from 0.1 to 5 Hz were also found in later measurements of artificial fogs with a lidar. In these measurements and those of Porch and Gillette, where the sampling rates were large enough to extend the PSDs to frequencies greater than 5 Hz, the slopes tended to flatten out at frequencies above that value.

A  $-5/3$  slope in the PSD has been observed for atmospheric aerosol backscatter using lidar measurements (Radkevich, et al., 2007). In backscattering measurements of this type—although aerosols of all sizes contribute to the signal—(i) the scattering efficiencies for particles much

smaller than the wavelength decrease rapidly as the size decreases; (ii) the scattering efficiencies for particles greater than about a wavelength are around two, and so the scattering cross-sections increase somewhat proportional to cross sectional area; and (iii) for a given particle cross-section, the backscattering by spherical aerosols is typically several times larger than for non-spheres with equivalent cross-sections. Because aerosols may be hygroscopic, the scattering from aerosols may increase rapidly as humidity increases, in ways that differ from changes in particle numbers in certain size ranges. The differences between the effects of humidity on backscattering and on particle numbers will depend upon the initial particle-size distribution, the thresholds chosen for counting particles, and on the wavelengths at which scattering is measured. In the measurements of Radkevich et al., (2007) the smallest sizes resolved are on the order of 3  $\mu$ m.

Single-particle statistics of atmospheric aerosol have been studied only to a limited extent. Following similar work with cloud droplets (e.g., Kostinski and Shaw 2001; Shaw et al. 2002) and precipitation (e.g., Kostinski and Jameson 1997; Larsen et al. 2005), most microphysical studies of aerosol particle number fluctuations have been conducted in the spatial domain rather than the PSD frequency domain (see, e.g., Preining 1983; Larsen et al. 2003; Larsen 2007). The discovery of non-trivial statistical spatial structure, however, suggests that the PSD could have non-trivial organized structure.

The statistics of atmospheric aerosols appears to be more complex than the statistics of atmospheric turbulence, defined in terms of wind velocities, for reasons such as the following.

- (a) Atmospheric aerosols in some size ranges and some situations probably act as passive scalars in the turbulent winds, and so it can be argued that they should have similarities in their statistical behavior, although the physical arguments for this may vary with the sources of aerosols.
- (b) The “aerosol concentration” may appear to be a continuously varying function of space and time when sample volumes are sufficiently large, but it is not continuous when the average number of particles in the sample volume is small or is less than one. The arrival times for such particles have been reported to deviate significantly from a Poisson distribution, at least for some cases (Larsen et al. 2003; Larsen 2007).
- (c) Aerosols diffuse much more slowly than gases (e.g., water vapor) or temperature (heat), and so mixing them should occur more slowly, especially in ranges where diffusive mixing is significant compared to convective mixing.
- (d) Atmospheric aerosols of different sizes may behave differently, largely because of gravitational settling rates and inertia. The largest particles may not follow the winds as well as typical “passive scalars” because their inertia is large, and their settling velocities may be much more significant.

- (e) Atmospheric aerosols may behave differently depending upon their composition and properties that depend upon composition. For example, ammonium sulfate particles increase in size as humidity increases. Particles differ in how well they may act as CCN. Those that are better as CCN may be washed out more rapidly.
- (f) Sources of aerosols (especially of non-water-droplet aerosols) may be more localized than are the sources of winds, in which the very large eddies have the most energy in power spectra. Example sources of aerosols are wind-blown dust from soil or other surfaces, such as the leaves of plants, or from plant debris; particles that are generated photochemically from vapor-phase terpenes emitted by plants; and combustion-generated particles from vehicular traffic, biomass burning, etc. The combustion emissions include particles such as fly ash or black carbon, which are emitted directly, but also low volatility molecules such as PAH, which are emitted as gasses at high temperature, but then condense onto the surface of other aerosols.
- (g) “Aging” of atmospheric aerosols is known to be important in modifying aerosols and their properties (Rudich). For example, organic compounds in aerosols may be oxidized by ozone and some of the products may be volatile, or they may be more hydrophilic and more efficient as CCN. Or, biological particles emitted into the atmosphere may become nonviable with time because of chemical reactions, which may be photochemical (e.g., formation of thymidine dimers in DNA) and/or may be with oxidizing molecules in the atmosphere (e.g., reactions of ozone with surface sugars on bacteria).

### **1.3 Approach**

Our primary objective in this report is to measure the aerosol concentrations, winds, and sonic temperature, and from these to calculate, in the inertial subrange, the slope of the PSDs of aerosol concentration and sonic temperature, as well as the fluctuations of the winds. We find that the calculated slope of the PSD of aerosols can be far different from the  $-5/3$  slope predicted in the inertial subrange even when the slopes of the PSDs of the winds and temperatures behave as predicted. We also find that the shot noise floor associated with sampling individual particles, with relatively small particle counts per bin, can limit the highest frequencies at which a  $-5/3$  slope is observed.

---

## **2. Methods**

---

### **2.1 Experimental**

The vector wind components ( $u$ ,  $v$ ,  $w$ ) and sonic temperature were measured using an RM Young Model 81000 sonic anemometer. The operational frequency of the anemometer is approximately 160 Hz with a maximum sampling frequency of 32 Hz. For this experiment, the anemometer was operated using a 20 Hz sampling frequency. The output data from the

anemometer is provided in ASCII text through an RS232 serial port. This output data was archived using a custom data acquisition system.

Particles were measured using a Climet Optical Particle Counter (OPC), (Climet, CI-8060). The particle scattering voltage versus time (as measured by a PMT inside the Climet) was recorded using a National Instruments data acquisition board run with LabVIEW. The PMT voltages, with time stamps, were subsequently processed to pick out peak heights and arrival times. Calibration of this system was accomplished using polystyrene latex spheres aerosolized with a nebulizer followed by a drying tube (Royco). Using this calibration, we selected a threshold of PMT voltage that corresponded to 0.85  $\mu\text{m}$  diameter PSL spheres (purchased from Duke Scientific). The particle counts were subsequently collected into 50 ms bins (20 Hz sampling) or 10 ms bins (100 Hz sampling).

The algorithm used to find the particle arrival times and peak heights employs a Schmitt trigger. Typically, when a particle is detected, the PMT voltage is high for around 5 to 15  $\mu\text{s}$ . The background voltage is assumed to have a noise that is small compared to the threshold voltage chosen. However, we have observed (as others have previously) that the “background” voltage of the OPC occasionally increases slowly (with rise times on orders of 10s to 100s of  $\mu\text{s}$ ) to voltages that may even exceed the threshold voltage. One possible reason for the slow increase in “background” may be that a particle is in a position where it moves slowly, but still scatters light that gets to the PMT. Another possible reason is that a very high concentration of (possibly small) particles entered the OPC. Cigarette smoke could possibly cause such an effect. This floating background could distort the particle statistics, for example, by appearing as extra particles with sizes above threshold, in cases where the “background” has floated to a significant fraction of threshold. If we do further work with the Climet OPC, we plan to develop more sophisticated algorithms to keep track of the “background” and count particles that have peak scattering that is greater than the sum of the background and the threshold chosen. Since—as best we can tell—these floating backgrounds are a relatively rare occurrence, we think that their effect on the statistics presented here is small. The discussion in the appendix on the effects of zeros in the particle counts adds to our impression that the effects of rare changes in particle counts are not so likely to cause large changes in the statistics.

The measurement site was the roof of Bldg 202 at the U.S. Army Research Laboratory (ARL) Adelphi Laboratory Center. The measurements were made for two periods: July 3–7 and July 13–17, 2007.

## **2.2 Analysis**

If the estimations of the PSDs are calculated directly from the data for aerosols, but also for winds and sonic temperatures, there are high frequency oscillations in the PSDs that are so large that it is difficult to discern where the underlying signal is. As described by Manolakis et al., (2000), in a section on estimating power spectra of stationary random signals, there are two main approaches to reducing the variance and smoothing the PSDs. These two approaches should

give similar results: (1) average the PSDs over frequency (e.g., by taking a running average), and (2) divide the input data into smaller ranges, compute PSD estimates for each of these, and then average the PSD estimates (the Welch or Welch-Bartlett method is an example of this approach). We calculated PSDs using both approaches (1) and (2), but then settled on approach (2) for the analysis shown here.

The PSDs for the aerosols, wind vector components, and sonic temperature were estimated using a modified Welch method. The modified Welch method computes an estimated PSD for a number of subwindows of the data being analyzed. Each subwindow is created using standard numerical filtering techniques such as a Hamming or Hanning window. The estimated spectral densities of each of these subwindows are then averaged to give the final estimated PSD. This technique tends to produce “smoother” spectra than does using a periodogram to estimate the spectral density. We employed the MATLAB routine *pwelch*, which implements the previously described method. By default, *pwelch* applies a Hamming window to eight overlapping segments of the input data. A second method used to provide an even smoother estimate of the PSD was implemented. This method also relied upon *pwelch*. The method makes successive calls to *pwelch*, using a smaller window size with each successive call. The lowest valid decade of frequency spectra are then saved. This procedure is repeated until the algorithm has covered all the viable frequency ranges.

The LabVIEW programs were written in such a way that there was a need to have some downtime to write the data to the hard drive. This time amounted to 1.5 s (30 samples of zero in the 20 Hz data) every 5 min, and two samples of unusable data (at 20 Hz) every 15 s. The appendix illustrates PSDs estimated using the Welch method for aerosols of July 13–17, 2007, with and without the zeros removed, and find that the effects on the PSD of removing these missing data points are small.

---

### 3. Results and Discussion

---

#### 3.1 Particle Counts Measured versus Time

The particle counts measured at Adelphi, MD, are shown in figure 1 for two sampling periods: July 3–7 and July 13–17, 2007. The peak particle count per 0.05 s bin was a little over 500. The average particles per 0.05 s bin was 33.4 and 29.4 for the two sampling periods, respectively.

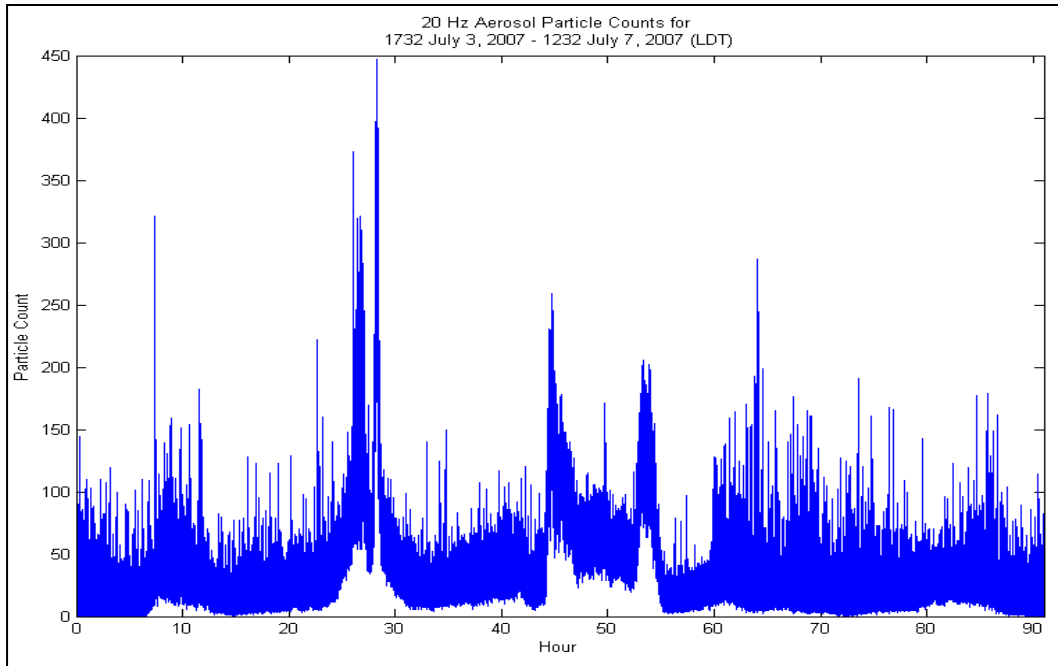


Figure 1a. Aerosol particle counts measured at 20 Hz using the Climet particle counter during the period July 3–7, 2007.

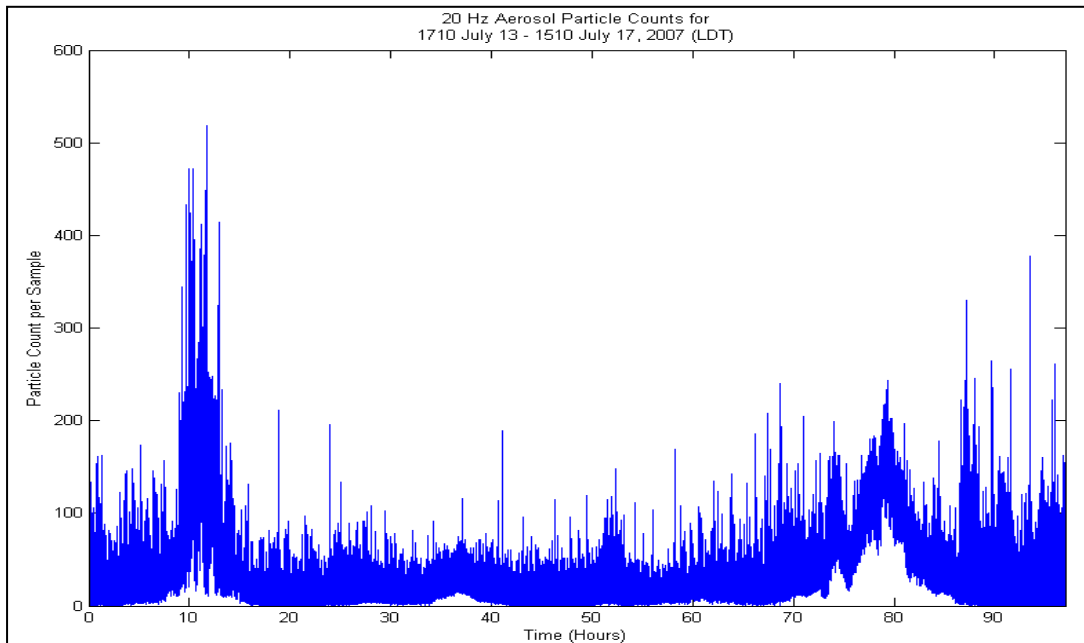


Figure 1b. Aerosol particle counts measured at 20 Hz using the Climet particle counter, July 13–17, 2007.

### 3.2 Power Spectral Densities of Wind, Temperature, and Aerosol for 90 h Periods

The PSDs of the winds ( $u$ ,  $v$ ,  $w$ ), temperature and aerosol concentration, all estimated using a modified Welch method, are illustrated in figure 2, which shows the data taken July 13–17, 2007. The curves have been normalized to have the same value at 0.2 Hz. The aerosol PSD is

calculated for the same data using two different sampling rates (20 Hz and 100 Hz). The inertial subrange, as defined by frequencies where the PSD of the winds decrease with a slope of  $-5/3$ , appears to be in the range 0.1 Hz to about 10 Hz. Although the slope of the temperature is close to  $-5/3$  in this range ( $10^{-1}$  to  $10^1$  Hz), the slope of the PSD of the aerosols is closer to  $-7/6$ . The next section discusses how a shot-noise floor might lead to flattened slopes of PSDs of aerosols.

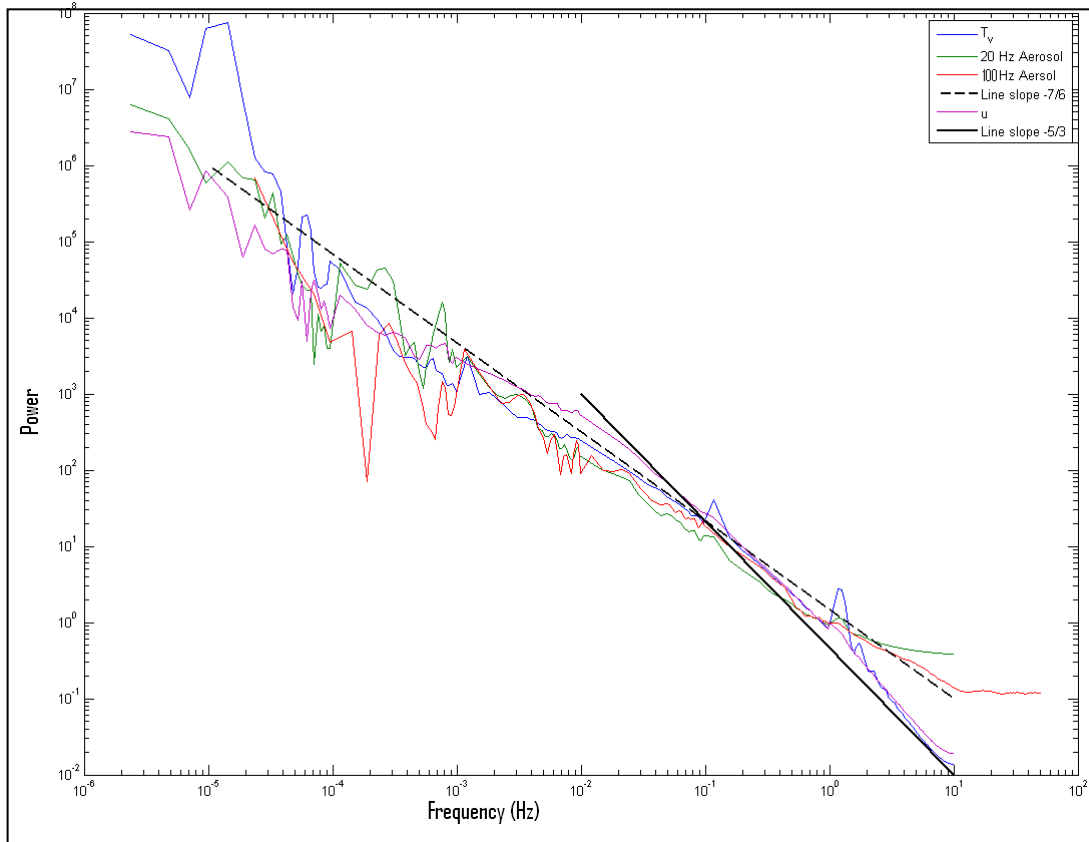


Figure 2. PSDs estimated using the modified Welch method for the  $u$  component of wind, the temperature ( $T_v$ ), and aerosols. The data for aerosols was binned into two different sampling frequencies before analysis. The lines with slopes of  $-5/3$  (solid) and  $-7/6$  (dashed) are for comparison with the winds and the aerosols, respectively. The slope of the wind ( $u$ ) is similar to  $-5/3$  in the inertial subrange ( $10^{-1}$  to  $10^1$  Hz).

The PSDs for the aerosols for the two sampling periods (July 3–7 and July 13–17, 2007) are illustrated in figure 3, without  $u$  and  $T_v$  to allow easier comparison. Both have a slope similar to  $-7/6$  in the range of about 0.0005 to 0.3 Hz. Below about 0.0005 there is an increase in the power in the July 3, 2007 data.

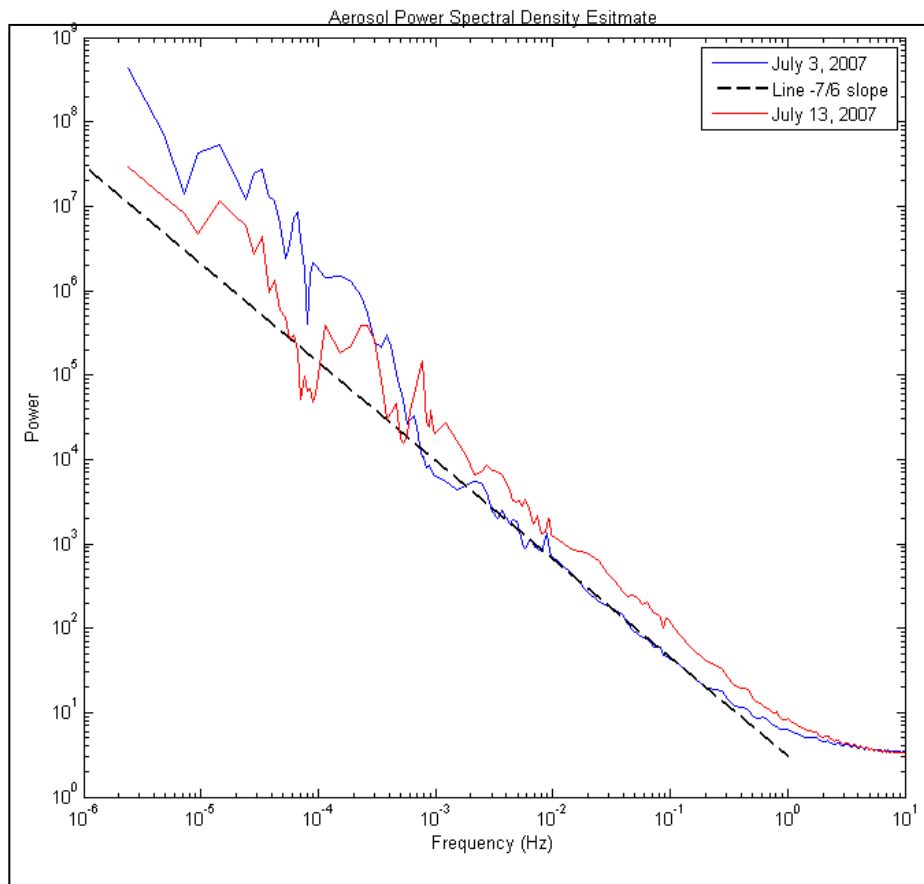


Figure 3. PSDs estimated using the modified Welch method for the aerosols for the two sampling periods (July 3–7 and July 13–17, 2007). The line with slope  $-7/6$  (dashed) is for comparison.

### 3.3 Limitations on Frequency Spectra as a Function of Particle Count (Shot Noise Floor)

At sufficiently low sample volumes and/or high sample rates, the number of aerosol particles (of whatever type or size range chosen for study) in a sample may become shot noise limited. Other passive scalars such as temperature, humidity, or concentrations of gases, are typically measured in terms of real numbers. They also have an upper frequency above which the power spectrum is resolution limited.

The PSD of a single delta function (or single particle at one instant of time) is flat. Also, the PSD of a sampled Poisson distribution with average number of  $N$  particles per sample is flat. It has power at the highest frequencies measured. For a Poisson distribution, the variance-to-mean ratio is 1.0, so if the average particle count per binned counting interval for the OPC is 100, the square root of the variance (the standard deviation) would typically be about 10.

To investigate the relations between particle counts and whether or not a  $-5/3$  slope could be observed, we picked a sample window that did have a  $-5/3$  slope, and then randomly omitted different fractions of the particles. The results are shown in figure 4.



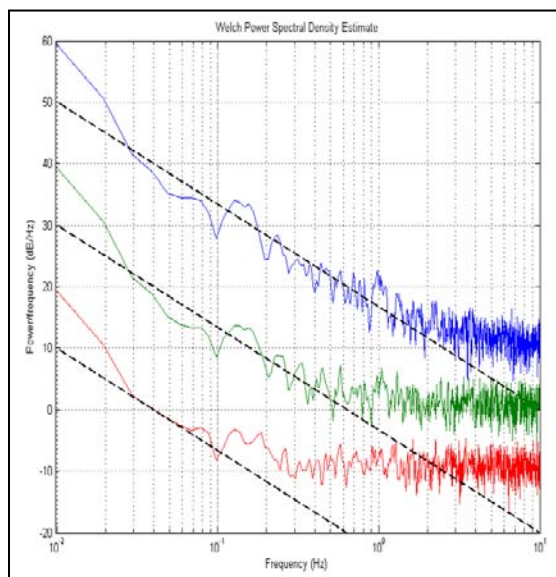


Figure 4. PSDs estimated for a 5-min sample of measured particles (blue) and for the sample after 90% (green) and then 99% (red) of the particles have been randomly eliminated.

One observation is that as the particle number decreases, the  $-5/3$  slope is maintained but only in a smaller frequency interval, one that includes the lowest frequencies. The frequency at which the line at  $-5/3$  bends to a slope near zero (i.e., the bend frequency”) moves toward lower frequencies as mean particle count decreases.

Also, as the particle count decreases by a factor of 10, the power in the low frequency region (where the slope is near  $-5/3$ ) decreases by a factor of  $10^2$ , as expected for cases with constructive interference between the Fourier components. On the other hand, the power in the high frequencies (where the slope is approximately zero) drops by a single decade, which is consistent with a Poisson distribution where the variance to mean ratio is one. That is consistent with the Fourier components having random phase relations with each other. These results have a similarity to mode-locking of a laser. When the laser is not locked, the fields of the modes have random phase relations to other modes. The energy output is constant in time and increases linearly with the number of modes that have a given energy. When the laser is mode-locked, the fields of the modes are all in phase at specific times, the fields add so that the total field at these specific times is  $N$  times larger than any one mode, and the power output, proportional to the field, squared, is  $N^2$  times as large.

One can imagine an appropriate averaging of curves like those in figure 4, generated with many different numbers of particles where the different curves have different “bend frequencies,” to obtain slopes that may be near linear, but with slopes much flatter than  $-5/3$ —e.g., with a slope of  $-7/6$ , as in figure 3.

### 3.4 Time-Dependence of the Slopes of the Power Spectral Densities of Wind, Temperature, and Aerosol for 5 min Intervals

The observation of  $-7/6$  slope for the aerosols raises questions about possible effects of shot noise (discussed in the next section) and the time variation of the slopes. Figure 5 shows the slope of the PSD of the wind  $u$  component, sonic temperature, and aerosol concentration for each 5 min interval of the 90 hr sampling period beginning July 3, 2007. Each slope was calculated for a 5 min interval, and the slope was determined by the computer for the PSD between 0.05 and 1 Hz. Each of these is shown versus time for the first 90 h of the measurement time.

Although the slopes of the PSDs of the wind and  $T_v$  are consistently near  $-5/3$  (within about 10%), the slopes of the PSDs of the aerosols vary from about  $-3/2$  to around 0.

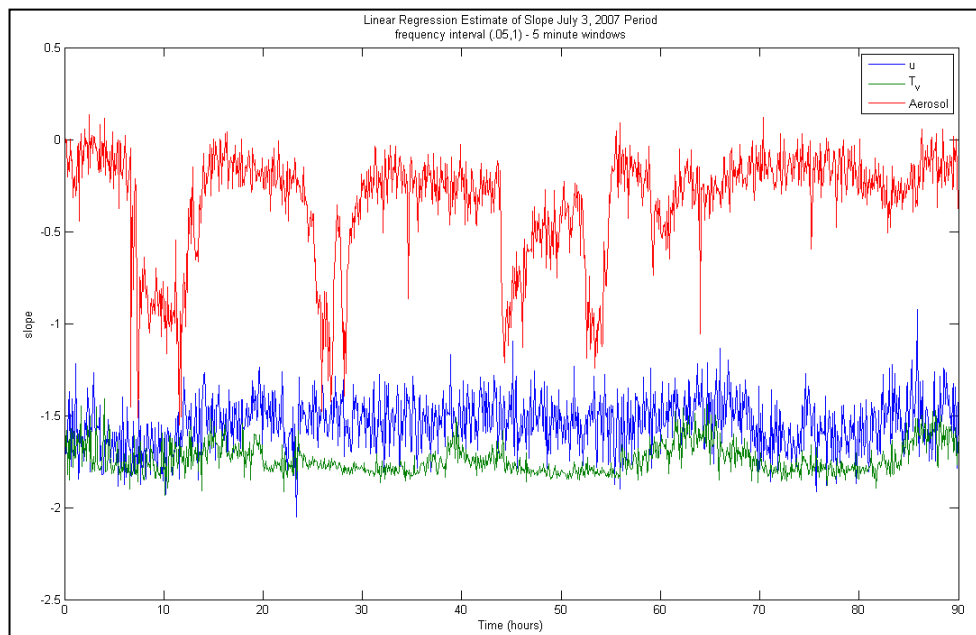


Figure 5. Estimate of the slope of the PSDs calculated for the winds (blue), sonic temperature (green), and aerosol number concentrations (red).

### 3.5 Slope of Aerosol Power Spectral Densities with Low and High Aerosol Concentrations

Figure 6 shows the mean aerosol particle count per bin, the TKE, and the slope of the aerosol PSD for each 5-min window of a 90 hr data collection beginning July 3, 2007. The times when the slopes of the aerosol PSDs are relatively large tend to occur when the particle numbers are larger. Correlations between the TKE and the slope of the aerosol PSD are not obvious.

Figure 7 shows the PSDs (estimated using the modified Welch method) of the aerosol particle concentrations measured at 20 Hz for the time periods illustrated in figure 4, in the July 3–7, 2007 data, where (a) is for the period where the concentration is low, and (b) is for the period from where the concentration is high. As expected from figure 4, the slope of the aerosol PSD

remains near  $-5/3$  over a much larger frequency range when the aerosol particle counts are high, as compared to when the aerosol particle counts are low.

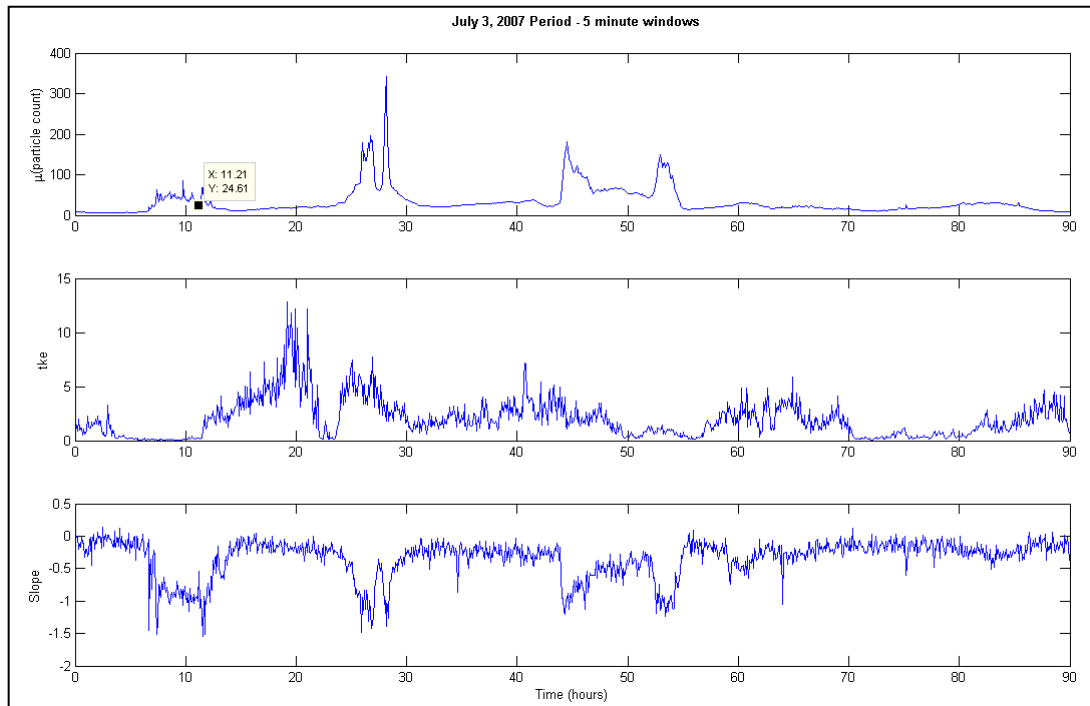


Figure 6. Mean particle count of aerosols, TKE, and slope of aerosol PSD for each 5-min window of a 90 hr data collection beginning July 3, 2007.

NOTE: Top: Average aerosol number per 50 ms sample period in the 5-min window. Middle: TKE for each window. Bottom: slope of PSDs (estimated using the modified Welch method) of the aerosol particle concentrations measured at 20 Hz.

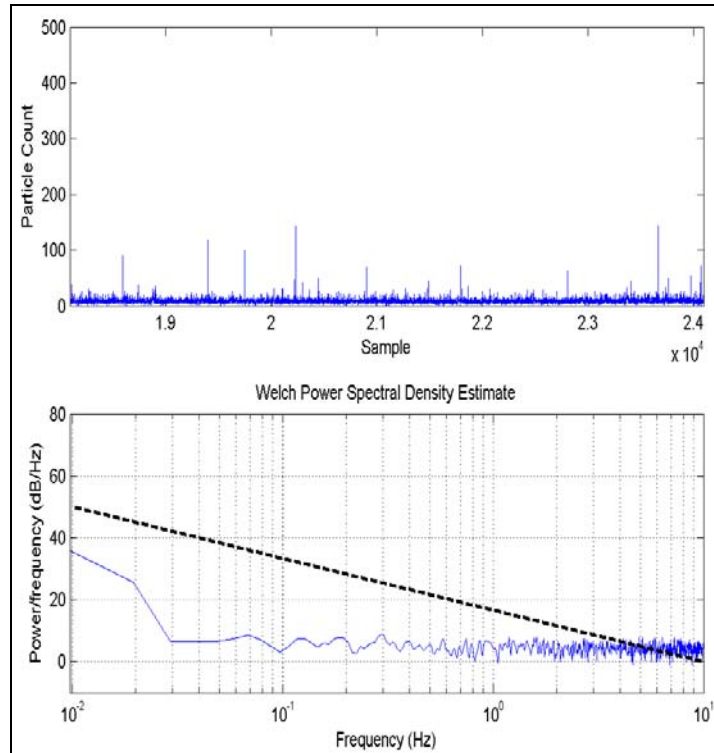


Figure 7a. Aerosol particle concentrations measured at 20 Hz using the Climet OPC, July 3–7, 2007, during a period where the concentration is lowest. The average particle count is about 9.21 per bin.

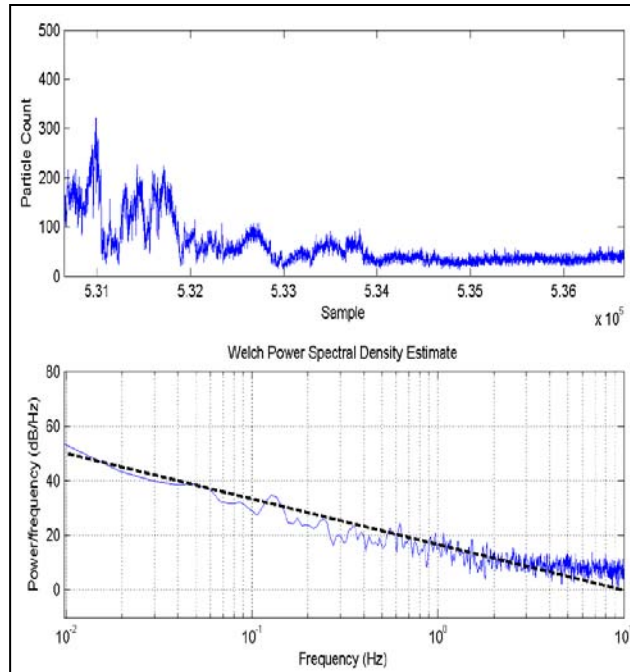


Figure 7b. Aerosol particle concentrations measured at 20 Hz using the Climet OPC, July 3–7, 2007, during a period where the concentration is highest. The average particle number is 62.8 per bin.

The mean particle count per bin required to observe an aerosol-PSD slope of a given magnitude is explored further in figure 8. Here, when the average particle count per bin is greater than 100 (for 6000 bins at 20 Hz), the slope can be within a few percent of  $-5/3$ . On the other hand, when the average particle count per bin is less than about 3, the slope is less negative than  $-0.5$ .

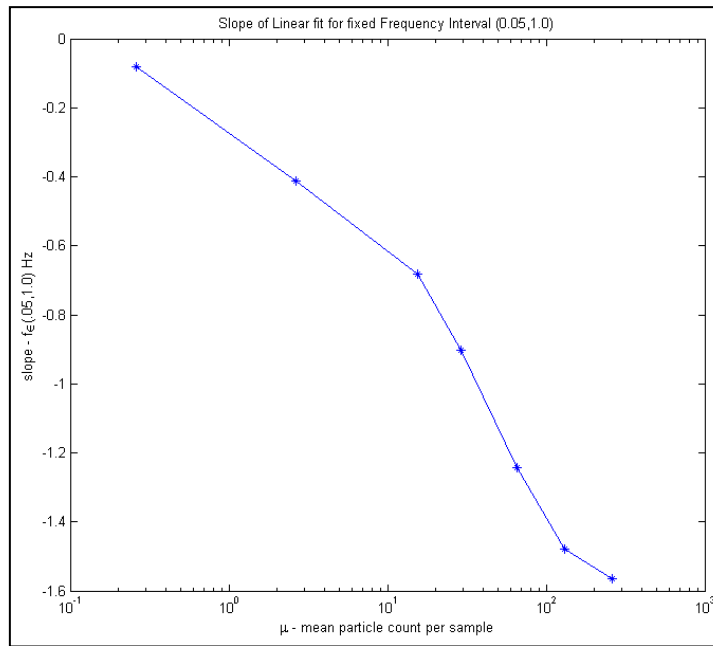


Figure 8. The slope of the linear fit of the PSD for a fixed frequency interval (0.05 to 1.0 Hz) and a given mean particle count.

Figures 9 and 10 investigate the size of the frequency interval, for which the linear fit of the PSD approximates a  $-5/3$  slope. Figure 9 indicates the right-hand bound of the interval, for which the fit is closest to a  $-5/3$  slope plotted against the mean particle count per bin. Figure 10 considers the largest intervals in which the slope of the linear fit is within 1%, 5%, or 10% of  $-5/3$ .

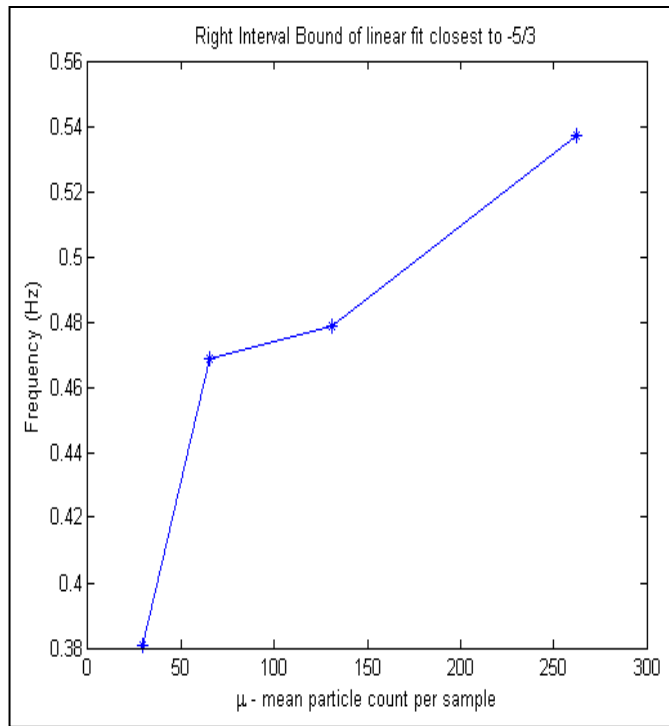


Figure 9. Right hand interval bound of the frequency interval for which the linear fit of the PSD was closest to  $-5/3$  slope, with a left hand bound of 0.05 Hz and a given mean particle count.

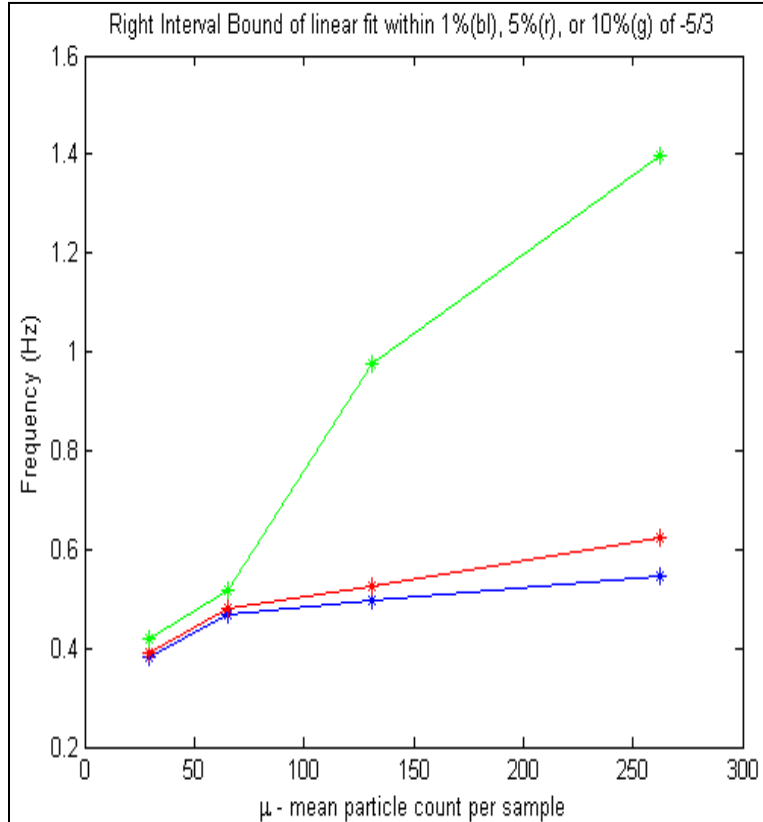


Figure 10. Right hand bound of the frequency interval for which the linear fit of the PSD is within 1% (blue), 5% (red), or 10% (green) of  $-5/3$  slope, with a left hand bound of 0.05 Hz and a given mean particle count.

---

## 4. General Discussion

---

The work presented here shows, to our knowledge, the first calculations of the PSDs of aerosol particle counts in the atmosphere. Previous PSDs of “aerosols” reported in the atmosphere were PSDs of aggregated scattering from all the particles in a volume (defined either by the scattering volume of the nephelometer (Porch and Gillette, 1977), or by the resolution of the lidar system (Radkevich, 2007), which contains many particles).

The aerosol particle count power spectrum may have more energy at higher frequencies, relative to the turbulence fluctuations of wind velocity or passive tracers, such as temperature or concentrations of added gases, especially if the air mass has had a long time to be away from its main sources of aerosols. If the air mass sample is many hours from the time the majority of the aerosols were injected, or many miles from the main sources of the aerosols in it, and, as this air mass moved, turbulence mixed and reduced the relative fluctuations in aerosol concentration,



then maybe the variations in aerosol concentration leftover from the turbulent mixing are still there, but are small relative to the Poisson variations.

Particles in an air mass might be distributed relatively homogeneously, if, for example, a large fraction of the aerosol in the air mass came from the Pacific Ocean or from photochemical generation of particles from gaseous OC, and the gaseous OC and the sunlight were relatively homogeneous. Consider an air mass in which turbulent mixing has occurred over a relatively long time after the sources have mostly stopped adding aerosol to the mass. For example, the source that was added was from a well-mixed tank of 0.5  $\mu\text{m}$  PSL mixed with SF<sub>6</sub>. The SF<sub>6</sub> and aerosols in it are then well-mixed by turbulent airflows and diffusion.

The measurable aerosol concentration depends upon the instrument. The smallest turbulent eddies studied in the atmosphere have sizes on the order of a few millimeters. (Stull, 1988, p.54).

---

## 5. Summary

---

Aerosol particle counts, winds, and temperature were measured on a rooftop in Adelphi for two 90-hr windows in July 2007. The particle counts were binned to 20 Hz and to 100 Hz. PSDs were calculated using modified Welch methods.

The slope of the aerosol PSD was observed to be about  $-7/6$  over 4 orders of magnitude, for each 4-day period. However, the slopes of the aerosol PSDs for each of the 5-min windows in the 90 hr periods were highly variable. Most of the slopes had magnitudes less than 0.5, and a large majority of the slopes had magnitude less than 1. Slopes near  $-3/2$  were very intermittent.

The frequency range in which a  $-5/3$  slope can be observed depends on the mean particle count per bin. The shot noise floor appears to dominate the PSDs when the observed particle counts were below roughly 30 particles per bin for time frames that have 6000 samples or 180,000 total particles.

Given the shot noise floor limitation of roughly 30 particles per bin at 20 Hz, we would like in future work to count as many aerosol particles as possible. Since the counting algorithm in this study was limited to aerosol particles that were 0.85  $\mu\text{m}$  and greater, a first step to address this limitation is to modify the algorithm to include in the count particles which are smaller. Such a modification to the algorithm would not necessarily be trivial using our CLIMET CI-8060, because the floating “background” issue discussed in section 2.1 would probably become more important. It may be easier to switch to a light scattering instrument that did not have any significant floating “background”.

---

## 6. References

---

- Batchelor, G. K. *The Theory of Homogeneous Turbulence* (Cambridge: 1953).
- Blackadar, A. K. *Turbulence and Diffusion in the Atmosphere* (Springer: 1997).
- Corrsin, S. On the Spectrum of Isotropic Temperature Fluctuations in an Isotropic Turbulence. *J. Appl. Phys.* **1951**, 22, 469–473.
- Eyink, G. L.; Sreenivasan, K. R. Onsager and the Theory of Hydrodynamic Turbulence. *Rev. Mod. Phys.* **2006**, 78, 87–135.
- Frisch, U. *Turbulence: the Legacy of A N Kolmogorov*, (Cambridge: 1995).
- Garvey, D. M.; Walters, D. L.; Fernandez, G.; Pinnick, R. G. 1982: Experimental Verification of the Kolmogorov Power Law from Aerosol Concentration Fluctuations. Proceeding, *Smoke/Obscurants Symposium*, Adelphi, MD.
- Hill, R. J. Implications of Monin-Obukhov Similarity Theory for Scalar Quantities. *J. Atmospheric Sciences* **1989**, 46, 2236–2244.
- Hill, R. J. Structure Functions and Spectra of Scalar Quantities in the Inertial-Convective and Viscous-Convective Ranges of Turbulence. *J. Atmospheric Sciences* **1989**, 46, 2245–2251.
- Jaenicke, R. Is Atmospheric Aerosol an Aerosol, *Faraday Discussions*, 2007.
- Kaimal, J. C. Turbulence Spectra, Length Scales, and Structure Parameters in the Stable Surface Layer. *Boundary-Layer Meteorol.* **1973**, 4, 289–309.
- Kaimal, J. C.; Wyngaard, J. C.; Izumi, Y.; Cote, O. R. Spectral Characteristics of Surface Layer Turbulence. *Quart. J. Roy. Meteorol. Soc.* **1972**, 98, 563–589.
- Kostinski, A. B.; Jameson, A. R. Fluctuation Properties of Precipitation. Part I: Deviations of Single Size Drop Counts from the Poisson distribution. *Journal of the Atmospheric Sciences* **1997**, 54, 2174–2186.
- Kostinski, A. B.; Shaw, R. A. Scale-dependent Droplet Clustering in Turbulent Clouds. *Journal of Fluid Mechanics* **2001**, 434, 389–398.
- Kundu, P. K. *Fluid Mechanics* (Academic: 1990).
- Larsen, M. L.; Cantrell, W.; Kostinski, A. B.; Kannosto, J. Detection of Spatial Correlations Among Aerosol Particles. *Aerosol Science and Technology* **2003**, 37, 476–485.
- Larsen, M. L.; Kostinski, A. B.; Tokay, A. Observation and Analysis of Steady Rain. *Journal of the Atmospheric Sciences* **2005**, 62, 4071–4083.

- Larsen, M. L. Spatial Distributions of Aerosol Particles. Investigation of the Poisson assumption. *Journal of Aerosol Science* **2007**, *38*, 807–822.
- Mandelbrot, B. B. Intermittent Turbulence in Self-similar Cascades: Divergence of High Moments and Dimension of the Carrier. *J. Fluid Mech.* **1974**, *62*, 331–358.
- Mandelbrot, B. B. *The Fractal Geometry of Nature*. (Freeman: New York). Ch. 10, 1977.
- Manolakis, D. G.; Ingle, V. J.; Kogan, S. M. 2000: *Statistical and Adaptive Signal Processing* (McGraw-Hill, Boston, MA), especially Ch. 5 and 5.3.
- Onsager, L. 1949: Statistical Hydrodynamics, Supplemento al volume VI, serie IX del Nuovo Cimento, *2*, 279–287.
- Porch, W. M.; Gillette, D. A. A Comparison of Aerosol and Momentum Mixing in Dust Storms Using Fast-Response Instruments. *J. Appl. Meteorology* **1977**, *16*, 1273–1281.
- Preining, O. Optical Single-particle Counters to Obtain the Spatial Inhomogeneity of Particulate Clouds. *Aerosol Science and Technology* **1983**, *2*, 79–90.
- Radkevich, A.; Lovejoy, S.; Strawbridge, K.; Schertzer, D. The Elliptical Dimension of Space-Time Atmospheric Stratification of Passive Admixtures Using Lidar Data, *Physica A* **2007**, *382*, 597–615. This paper cites several other papers from the Schertzer-Lovejoy group that have PSDs from lidar measurements of scattering by aerosols.
- Shaw, R. A.; Kostinski, A. B.; Larsen, M. L. Towards Quantifying Droplet Clustering in Clouds. *Quarterly Journal of the Royal Meteorological Society* **2002**, *128*, 1043–1057.
- Tennekes, H.; Lumley, J. L. *A First Course in Turbulence* (MIT Press: Cambridge, MA), 1972.
- Tung, K. K.; Orlando, W. W. The k-3 and k-5/3 Energy Spectrum of Atmospheric Turbulence: Quasigeostrophic Two-Level Model Simulation. *J. Atmospheric Sciences* **2003**, *60*, 824–835.
- Van Etten, W.; van der Plaats, J. *Fundamentals of Optical Fiber Communications* (Prentice Hall: New York).
- Warhaft, Z. Passive Scalars in Turbulent Flows. *Annu. Rev. Fluid Mech.* **2000**, *32*, 203–240.
- Wheeler, A. D. On the Spectrum of a Passive Scalar Mixed by Turbulence. *J. Geophys Res* **1958**, *63*, 849–850.

INTENTIONALLY LEFT BLANK.

---

## Appendix. Effect of Dropping 15 s of Data

---

Due to the way the aerosol particle data were collected in order to investigate longer time periods than 5 min, the data needed to be concatenated. Two methods for this concatenation are time preserving zero padding and strict concatenation (ignore the 1.5 s of missing data). As can be seen in figures A-1 and A-2, there is not a significant structural difference in the PSD estimate between the two methods. However, in order to compare with the continuous data provided by the sonic anemometer, it is preferred to adopt the time preserving method.

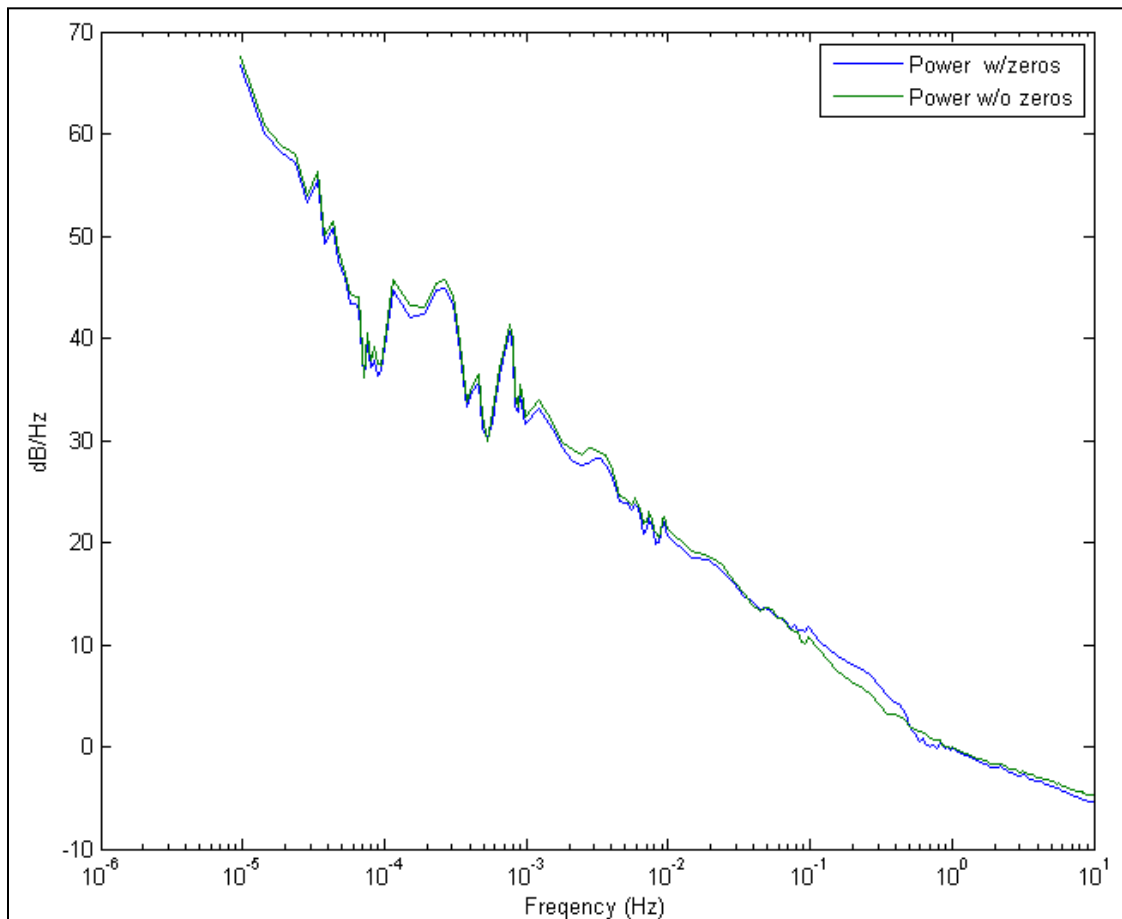


Figure A-1. PSDs for aerosols July 13–17, 2007, with and without the zeros removed. The effect appears small.

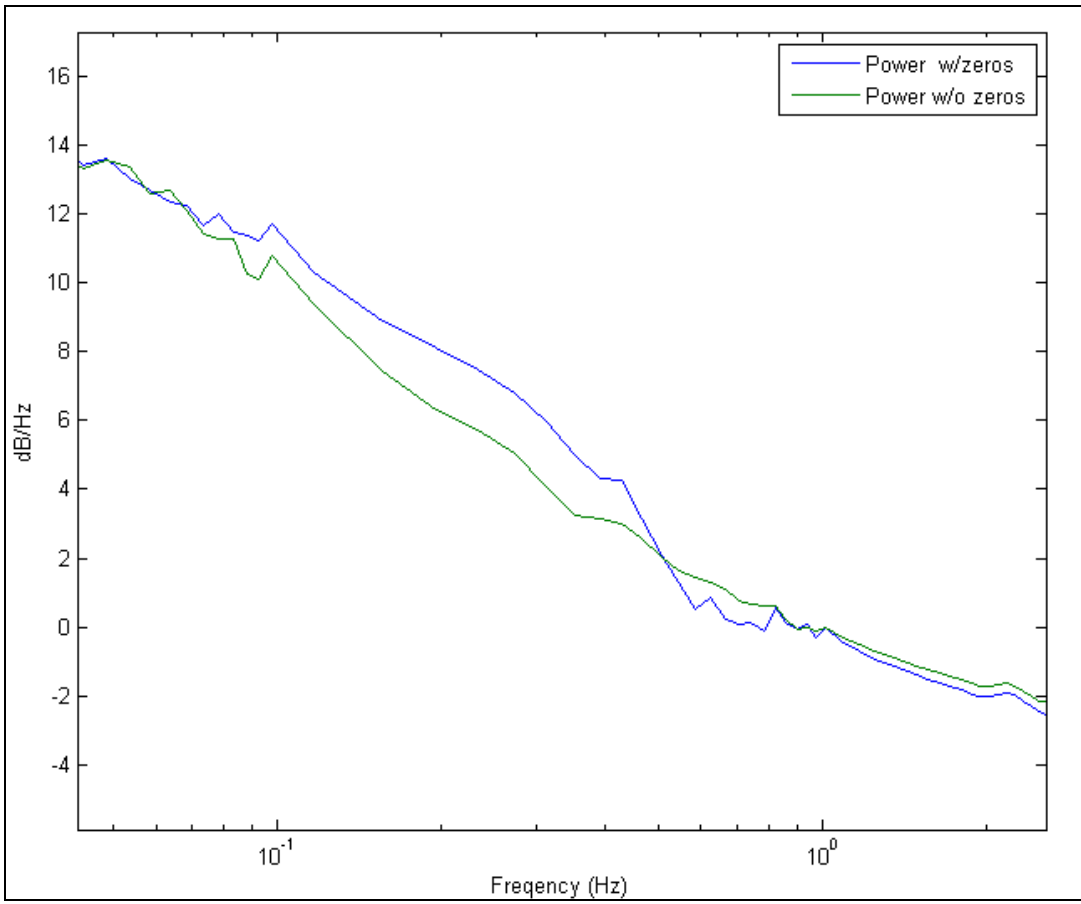


Figure A-2. Same as for figure A-1 though limiting the display to the frequency interval in the region of most significant difference for the two PSDs.

NO. OF COPIES	ORGANIZATION	NO. OF COPIES	ORGANIZATION
1 ELECT	ADMNSTR DEFNS TECHL INFO CTR ATTN DTIC OCP 8725 JOHN J KINGMAN RD STE 0944 FT BELVOIR VA 22060-6218	1	US ARMY RSRCH LAB ATTN RDRL CIM G T LANDFRIED BLDG 4600 ABERDEEN PROVING GROUND MD 21005-5066
1	DARPA ATTN IXO S WELBY 3701 N FAIRFAX DR ARLINGTON VA 22203-1714	1	DIRECTOR US ARMY RSRCH LAB ATTN RDRL ROE V W D BACH PO BOX 12211 RESEARCH TRIANGLE PARK NC 27709
1 CD	OFC OF THE SECY OF DEFNS ATTN ODDRE (R&AT) THE PENTAGON WASHINGTON DC 20301-3080	16	US ARMY RSRCH LAB ATTN IMNE ALC HRR MAIL & RECORDS MGMT ATTN RDRL CIE D C WILLIAMSON (10 COPIES) ATTN RDRL CIE D D GARVEY ATTN RDRL CIE D C KLIPP ATTN RDRL CIE S S HILL ATTN RDRL CIM L TECHL LIB ATTN RDRL CIM P TECHL PUB ADELPHI MD 20783-1197
1	US ARMY RSRCH DEV AND ENGRG CMND ARMAMENT RSRCH DEV & ENGRG CTR ARMAMENT ENGRG & TECHNLOGY CTR ATTN AMSRD AAR AEF T J MATTS BLDG 305 ABERDEEN PROVING GROUND MD 21005-5001	TOTAL: 26 (24 HCS, 1 ELECT, 1 CD)	
1	PM TIMS, PROFILER (MMS-P) AN/TMQ-52 ATTN B GRIFFIES BUILDING 563 FT MONMOUTH NJ 07703		
1	US ARMY INFO SYS ENGRG CMND ATTN AMSEL IE TD A Rivera FT HUACHUCA AZ 85613-5300		
1	COMMANDER US ARMY RDECOM ATTN AMSRD AMR W C MCCORKLE 5400 FOWLER RD REDSTONE ARSENAL AL 35898-5000		
1	US GOVERNMENT PRINT OFF DEPOSITORY RECEIVING SECTION ATTN MAIL STOP IDAD J TATE 732 NORTH CAPITOL ST NW WASHINGTON DC 20402		

INTENTIONALLY LEFT BLANK.